Heliyon 9 (2023) e22282

Contents lists available at ScienceDirect

Heliyon

journal homepage: www.cell.com/heliyon

Upregulation of miR-194-5p or silencing of PRC1 enhances radiotherapy sensitivity in esophageal squamous carcinoma cells

Yan Wang, Ninghua Yao, Jie Sun *

Department of Radiotherapy, Affiliated Hospital of Nantong University, Nantong, 226001, Jiangsu, PR China

ARTICLE INFO

Keywords:
miR-194-5p
PRC1
Wnt/β-catenin
Esophageal squamous cell carcinoma
Radiotherapy sensitivity
Invasion
Metastasis

ABSTRACT

Background: To investigate the possible molecular mechanism of miR-194-5p/PRC1/Wnt/β-catenin signaling axis that regulates the invasive metastatic ability and radiotherapy sensitivity of esophageal squamous cell carcinoma (ESCC) cells.

Methods: ESCC-related differentially expressed miRNAs were identified by microarray analysis, followed by the identification of a putative target. The targeting relationship between miR-194-5p and PRC1 was assayed. A series of mimic and shRNA were transfected into ESCC cells to find out the mechanism of miR-194-5p in ESCC by regulating PRC1 through Wnt/β-catenin signaling pathway and their effect on cell proliferation, migration, invasion, and radiosensitivity as well as xenograft tumor growth and metastasis in nude mice.

Results: We demonstrated low miR-194-5p expression and high PRC1 expression in ESCC tissues and cells. PRC1 was confirmed as a putative target for miR-194-5p. High miR-194-5p or silenced PRC1 enhanced ESCC cell radiosensitivity but reduced proliferation, invasion, and migration via PRC1 through modulation of the Wnt/β-catenin signaling pathway. Animal experiments also validated that overexpression of miR-194-5p suppressed tumorigenesis and in vivo metastasis in nude mice.

Conclusion: miR-194-5p can inhibit the Wnt/β-catenin signaling pathway through down-regulation of the PRC1 gene, thereby enhancing the sensitivity of ESCC cells to radiotherapy and attenuating the invasion and metastasis ability of ESCC cells.

1. Introduction

Esophageal cancer is a severe malignancy and is one of the most common cancers worldwide [1]. Esophageal squamous cell carcinoma (ESCC), a subtype of esophageal cancer, accounts for approximately 90 % of esophageal cancers and is commonly found in East Asia and Africa [2]. Studies have shown that ESCC occurs through the malignant transformation of esophageal epithelial cells, and its lesions are mainly found in the middle esophagus [3]. Various well-characterized risk factors, such as smoking, excessive alcohol consumption, and salted vegetables, have contributed to the high incidence of ESCC [4]. Although some progress has been made in diagnosis and treatment, its metastatic and invasive capacity remains a significant difficulty in current treatment [5]. Radiotherapy has been widely used as an essential tool in treating esophageal cancer [6]. However, tumor cells tend to develop resistance to radiotherapy, which is one of the key factors slowing down the therapeutic effect [7]. Several studies have shown that some miRNAs'

* Corresponding author. Department of Radiotherapy, Affiliated Hospital of Nantong University, No. 20, Xishi Road, Nantong, 226001, Jiangsu Province, PR China.

E-mail address: ntsunjie90@163.com (J. Sun).

https://doi.org/10.1016/j.heliyon.2023.e22282
Received 31 July 2023; Received in revised form 8 November 2023; Accepted 8 November 2023
Available online 13 November 2023

aberrant expression is associated with tumor cells' sensitivity to radiotherapy [8].

In recent years, miRNAs have been widely studied as targets for cancer therapy [9]. Specific miRNAs have been found to have regulatory roles in tumor immunotherapy by influencing the expression levels of immune checkpoint molecules and modulating the immune evasion capability of tumor cells towards T cells [10,11]. Also, studies have shown that aberrant expression of miRNAs is essential in the development and progression of esophageal cancer [12]. miR-194-5p is an isoform of miR-194 that is aberrantly expressed in various cancers, including esophageal [13]. Although several studies have reported the role of miR-194-5p in esophageal cancer, the molecular mechanism by which it regulates esophageal cancer cell invasion and metastasis remains unclear [13].

Polycomb complex 1 (PRC1) is a critical epigenetic modifier that regulates gene expression [14]. Although aberrant expression of PRC1 has been reported in various cancers, its role in esophageal cancer still needs further investigation [15]. Meanwhile, high expression of PRC1 in hepatocellular carcinoma promotes tumor cell proliferation and tumorigenesis through activation of the Wnt/β-catenin pathway [16]. In the Wnt/β-catenin signaling pathway, β-catenin is a critical transcription factor that affects cell proliferation and transformation [17]. Several studies have shown that aberrant expression of β-catenin in various cancers is closely associated with tumor invasion and metastasis [18]. Aberrant expression of β-catenin has also been reported in esophageal cancer [18]. However, it is unclear how miR-194-5p regulates β-catenin expression in esophageal cancer and its effect on tumor cell invasion and metastasis [19].

This study aimed to investigate the molecular mechanism of miR-194-5p/PRC1/Wnt/β-catenin signaling axis on the invasive metastatic ability and radiotherapy sensitivity of ESCC cells. We demonstrated that miR-194-5p could inhibit the Wnt/β-catenin signaling pathway by down-regulating PRC1, thus enhancing the sensitivity of ESCC cells to radiotherapy and weakening the invasion and metastasis of ESCC cells, which is expected to provide new ideas and methods for the clinical diagnosis and treatment of ESCC.

2. Materials and methods

2.1. Clinical sample collection

Sixty specimens of ESCC tissues (all patients had not undergone chemotherapy or radiotherapy before surgery and had not taken hormonal drugs) were surgically resected in our hospital from January 2016 to December 2016. The paracancerous tissues surrounding the ESCC tissues were also excised (to form a control with the carcinoma tissues), and all specimens were stored in a refrigerator at −80 °C for backup. All patients signed an informed consent form, which our clinical ethics committee approved and agreed upon, and all specimens were used following the Declaration of Helsinki.

2.2. Bioinformatics analysis

Using the GEO database (https://www.ncbi.nlm.nih.gov/geo/), the ESCC miRNA expression microarray dataset GSE97051 was obtained, including 7 standard esophageal and 7 ESCC tissue samples. Differential analysis was performed by the R language "limma" package with |logFC|>12, p-value <0.05 as the screening criteria for differentially expressed genes. The MNDR database (http://www.rna-society.org/mndr/, version v3.1, screening condition: Species = *Homo sapiens* & Score>0.7) was used to search the keyword "esophagus squamous cell carcinoma" to obtain relevant miRNAs. The jvenn tool (http://jvenn.toulouse.inra.fr/app/example.html) was used to find overlaps of differentially underexpressed miRNAs and MNDR database results.

The StarBase database (http://starbase.sysu.edu.cn/), miRDB database (http://mirdb.org/), and RNA22 database (https://cm.jefferson.edu/rna22/Precomputed/) were searched to query the downstream target genes of miRNA. The jvenn tool (http://jvenn.toulouse.inra.fr/app/example.html) was screened to find the overlap of miRNA targets in each database. The GeneCards database (https://www.genecards.org/) was used to search the keyword "esophagus squamous cell carcinoma" to obtain the top 2000 related genes in Score.

The RNAseq data in TPM (transcripts per million reads) format of TCGA and GTEx were obtained from the UCSC XENA database (https://xenabrowser.net/datapages/), and the expression comparison between samples was performed after log2 transformation. ESCC in TCGA and the corresponding average tissue data in GTEx were extracted, and 666 standard samples and 182 ESCC samples were finally obtained. Statistical analysis was performed on the differential expression of candidate genes using the Mann-Whitney *U* test (Wilcoxon rank sum test), and the difference was considered significant when $p < 0.05$. The R language "ggplot2" package (https://www.rdocumentation.org/packages/ggplot2/versions/3.3.0) was used to draw gene expression boxplots.

2.3. Dual-luciferase reporter gene assay

Briefly, PRC1 3′-UTR-wild-type (WT) and PRC1 3′-UTR-mutant (Mut) were inserted into pMIR-reporter (AM5795, Invitrogen™). After that, the luciferase reporter plasmids (PRC1-WT and PRC1-Mut) were co-transfected with negative control and miR-194-5p, respectively, into human embryonic kidney (HEK-293T) cells (BNCC353535, BeNa culture collection, Suzhou, China) for 48 h. Dual-luciferase activity was finally analyzed using a luciferase assay kit (RG005, Beyotime Biotechnology Co., Ltd., Shanghai, China).

2.4. TOP/FOP flash dual luciferase reporter gene assay

KYSE150 cells in the logarithmic growth phase were inoculated in 12-well cell culture plates at a concentration of 1×10^5/mL one day before transfection, and the liposome transfection experiment was performed when the cell density grew to 70–80 %. The TOP

Flash plasmid (D2501, Shanghai Biyuntian Biotechnology Co., Ltd., Shanghai, China) (or FOP Flash control plasmid (D2503, Shanghai Biyuntian Biotechnology Co., Ltd., Shanghai, China)) and mimic NC, miR-194-5p mimic, sh-NC, and sh-PRC1 were transfected for 48 h. The cells were collected and lysed. The cells were centrifuged for 3–5 min, the supernatant was extracted, and the luciferase activity was detected using the luciferase assay kit (RG005, Shanghai Biyuntian Biotechnology Co., Ltd., Shanghai, China). In addition, 100 μL of firefly dual luciferase working solution was added to each cell sample to detect firefly dual luciferase (Firefly luciferase), and 100 μl of sea kidney dual Renilla luciferase was added to each cell sample to detect Firefly luciferase and Renilla luciferase as the relative dual luciferase activity.

2.5. Cell culture, transfection, and grouping

ESCC cell line KYSE150 (CL-0638) was purchased from Procell Life Science&Technology Co., Ltd. (Wuhan, Hubei, China), and human esophageal epithelial cell HET-1A (CRL-2692) was procured from ATCC (Rockville, MD, USA). All cells were cultured with Roswell Park Memorial Institute (RPMI)-1640 medium (11875119, Gibco) containing 10 % fetal bovine serum (FBS, 16140071, Gibco) in an incubator containing 5 % CO2 under saturated humidity condition at 37 °C. Cells in the logarithmic growth phase were seeded in 6-well plates (3×10^5/mL per well). Upon reaching 90 % confluence, the KYSE150 cells were transfected with the plasmids from Dharmacon (Lafayette, CO, USA), including miR-194-5p mimic, sh-PRC1, oe-PRC1 or corresponding controls with the utilization of Lipofectamine 2000 (11668019, Thermo Fisher). Following 6-h transfection, cells were cultured in a complete medium for another 48 h, and finally, cells were collected.

2.6. Cell irradiation method

The KYSE150 cells were trypsinized and dissociated into a single-cell suspension, with cell concentration calculated. After cell inoculation (1×10^6 cells/well) in 6-well plates for 12 h, the cells covered with plexiglass filler (1 cm) were irradiated with a 6-MV x-ray beam at a radiation dose of 3 gamma-rays (Gy/min) from Varian-2300EX linear accelerator (Varian Medical Systems, Inc., USA) (source skin distance: 100 cm; filed size: 10 cm × 10 cm.

2.7. Clonogenic assay to detect sensitivity to radiotherapy

The KYSE150 cells were detached with trypsin (0.25 %), dissociated into single-cell suspension, centrifuged, and added RPMI-1640 medium supplemented with 10 % FBS. Cells were then seeded in 6-well plates (1×10^3 cells per well). Following 24-h incubation, cells were exposed to radiation of different doses (0 Gy, 2 Gy, 4 Gy, 6 Gy, 8 Gy, and 10 Gy) and incubated in a 5 % CO2 incubator at 37 °C for a week. The culture medium was changed every two days. When clones were visible at the bottom of the well, the culture was stopped, and cells were washed, fixed with methanol (2 mL) for 20 min, and stained with Giemsa solution (2 mL, G4640, Solarbio; 40 min) followed by microscopic observation (IX-50, Olympus, Japan) for counting number of a colony with no less than 50 cells. Then, the planting efficiency (PE) and the surviving fraction (SF) were calculated: PE = (the number of clone formations under different radiation doses/number of incubated cells) × 100 %; SF = (number of clone formation following irradiation/number of incubated cells × PE) × 100 %. A cell survival curve was constructed by GraphPad Prism 6.0 software (GraphPad Software, CA, USA).

2.8. CCK-8 method

The KYSE150 cells from each group were washed twice with PBS after 48 h of transfection. 0.25 % trypsin digested the cells and then centrifuged at 1000 rpm for 5 min. The cells were blown with a pipette gun to make a uniform single-cell suspension. Cells were inoculated in 96-well plates with 2.5×10^3 cells per well and incubated at 37 °C in a 5 % CO2 incubator. Three replicates were set up for each well. After 24 h, 48 h, and 72 h of incubation, 10 μL of CCK-8 reagent (C0037, Shanghai Biotechnologies Co., Ltd., Shanghai, China) was added to each well. After mixing, incubation was continued at 37 °C in a 5 % CO2 incubator for 2 h. Each well's absorbance (OD) values were detected at 450 nm by an automated enzyme reader (51119180 ET, MultiskanTM FC, Thermo, Waltham, MA, USA). The cell growth curve was plotted after setting the average OD value of each group as the vertical coordinate and the time as the horizontal coordinate to calculate the cell growth viability.

2.9. Scratch test

The KYSE150 cells from each group at 48 h after transfection were digested with 0.25 % trypsin and blown into a single cell suspension for cell counting, and then inoculated in 6-well plates at a density of 1×10^6/well with careful shaking and mixing after 24 h of incubation in complete medium, the culture was changed to RPMI1640 medium containing 10 % fetal bovine serum. Use a sterile 200 μL micropipette tip to score perpendicular to the horizontal line behind and wash 3 times with PBS to remove cells dislodged by disruption of the pipette tip; add serum-free medium and incubate at 37 °C with 5 % CO_2 incubator. Photographs were taken at 0 h and 24 h for observation under the microscope.

2.10. Transwell assays for cellular invasion

A final 1 mg/mL concentration of Matrigel (E6909, Sigma-Aldrich, USA) was prepared with precooled serum-free RPMI-1640 medium. Then, the diluted matrigel (80 μL per well) was put into the apical chamber of each Transwell chamber (8 μm) and incubated at 37 °C for 4 h. Following the 48-h transfection, cells were suspended using serum-free RPMI-1640 medium and adjusted to a 1×10^6/mL density, then added to the apical chamber. RPMI-1640 medium (700 μL) with 10 % FBS was added to the basolateral chamber (bottom of the 24-well plate). Following 24 h of incubation, the cells in the apical chamber were fixed with paraformaldehyde (4 %) and stained for 30 min with 0.05 % crystal violet at room temperature. Finally, with 10 visual fields randomly selected, the cells were counted after microscopic observation (XSP-8CA, Shanghai Optical Instrument Factory, Shanghai, China).

2.11. Cell cycle detection by flow cytometry

KYSE150 cells were collected after 48 h of transfection and other treatments, digested with 0.25 % trypsin to make a single cell suspension, washed twice with PBS, centrifuged, and the supernatant discarded. Add pre-cooled 70 % ethanol and fix overnight at 4 °C. Cells were resuspended by reshaking, centrifuged, and washed twice with pre-chilled PBS, resuspended in 100 μL of PBS, RNase was added to a final concentration of 1 mg/mL, and water bath at 37 °C for 30min. The PI staining solution was added to a final concentration of 50 μg/mL and stained at 4 °C for 40 min, protected from light, followed by PBS washing, and the cell cycle was detected at >575 nm. DNA content and cell cycle percentage were calculated.

2.12. RT-qPCR

At 48 h after transfection, KYSE150 cells were collected from each group. Total RNA was extracted using the Trizol (15596026, Invitrogen, Car, Cal, USA) method, and RNA integrity was identified by 1 % agarose gel electrophoresis, and RNA concentration and purity were measured by Nano-Drop ND-1000 spectrophotometer. The cDNA template was synthesized by reverse transcription reaction in a PCR amplifier according to the reverse transcription kit instructions (AU341-02, purchased from Beijing All-Style Gold, Beijing, China), and primers for miR-194-5p, PRC1, β-catenin, Cyclin D2, C-myc, MMP-2, and GADPH were designed and synthesized by Shanghai Biotech (Table S1). The reverse transcription experimental system was 20 μL, referring to the instructions of EasyScript First-Strand cDNA Synthesis SuperMix (Catalog No. AE301-02, Beijing All-Style Gold). The reaction solution was taken for real-time fluorescence PCR, and the fluorescence PCR operation was performed by referring to the instructions of TB Green® Premix Ex Taq™ II (Tli RNaseH Plus) (RR820L, TaKaRa, Dalian, China). The reaction system was 20 μL: 10 μL SYBR Premix, 2 μL cDNA template, upstream and downstream. The reaction system was 20 μL: 10 μL SYBR Premix, 2 μL cDNA template, 0.6 μL each upstream and downstream primers, and 6.8 μL DEPC water. The conditions were: pre-denaturation at 95 °C for 30 s, denaturation at 95 °C for 30 s, annealing for 20 s, extension at 72 °C for 30 s and 40 cycles to detect the expression levels of miR-194-5p, PRC1, β-catenin, Cyclin D1, C-myc, MMP-2, and GADPH. The 2-ΔΔCt method was applied for gene expression analysis.

2.13. Western blot

The KYSE150 cells of each group after 48 h of transfection culture were collected, washed with PBS and resuspended. The supernatant was removed by centrifugation, and RIPA lysate (P0013B, Biyuntian Biotechnology Co., Ltd., Shanghai, China), an appropriate amount of PMSF (phenylmethylsulfonyl fluoride), and phosphatase inhibitor were added at the ratio of 1 mL per 107 cells, and then incubated on ice for 30 min, centrifuged at 12000 rpm, 4 °C for 10 min, and the supernatant was removed, which was the total cell protein. The protein concentration was determined using the Beyoncé BCA Protein Quantification Kit (P0012S, Beyoncé Biotechnology Co., Ltd., Shanghai, China) and adjusted to 4 μg/μL with PBS. 30 μg of total cellular protein was subjected to SDS-PAGE, followed by wet transfer to NC membrane and closed with 5 % skim milk powder (prepared by TBST) for 1.5 h. According to the antibody instructions The corresponding antibodies were diluted in primary antibody dilutions of PRC1 (rabbit anti-human, ab51248, 1:10,000), β-catenin (rabbit anti-human, ab32572, 1:5000–1:10,000), p-β-catenin (rabbit anti-human, ab27798, 1:500), Cyclin D1 (rabbit anti-human ab134175, 1:10000–1:50000), C-myc (rabbit anti-human, ab32072, 1:10000), MMP-2 (rabbit anti-human, ab92536, 1:1000–1:5000), GAPDH (rabbit anti-human, ab9485, 1:2500) above were obtained from Abcam, UK. the closed NC membranes were placed in plastic dishes, and the above antibodies were added separately and placed at 4 °C and shaken overnight. The next day, the membranes were rinsed with TBST for 15 min × 3 times. Add diluted HRP-labeled secondary antibody IgG (goat anti-rabbit, ab205718, 1:2000–1:50000) in the same way, incubate for 2 h at room temperature, and then wash the membrane with TBST for 15 min × 3 times. Put into ECL luminescent solution for color development, and SmartView Pro 2000 (UVCI-2100, Major Science, USA) was photographed. The protein bands were analyzed in grayscale using Quantity One software version 4.52 [20].

2.14. In vivo animal studies

Sixty-four 5-week-old female BALB/c nude rats, weighing 18–20 g, were purchased from the Shanghai Experimental Animal Center of the Chinese Academy of Sciences and housed in an SPF-grade laboratory room at constant temperature (25 ± 2) °C and humidity (45%–50 %) with a 12-h dark/light cycle, fed autoclaved standard laboratory chow and free sterile drinking water. All experimental operations followed the International Convention on Laboratory Animal Ethics and met relevant national regulations. KYSE150 cells in the logarithmic growth phase in the corresponding groups after transfection (mimic NC group, miR-194-5p mimic group, miR-194-5p

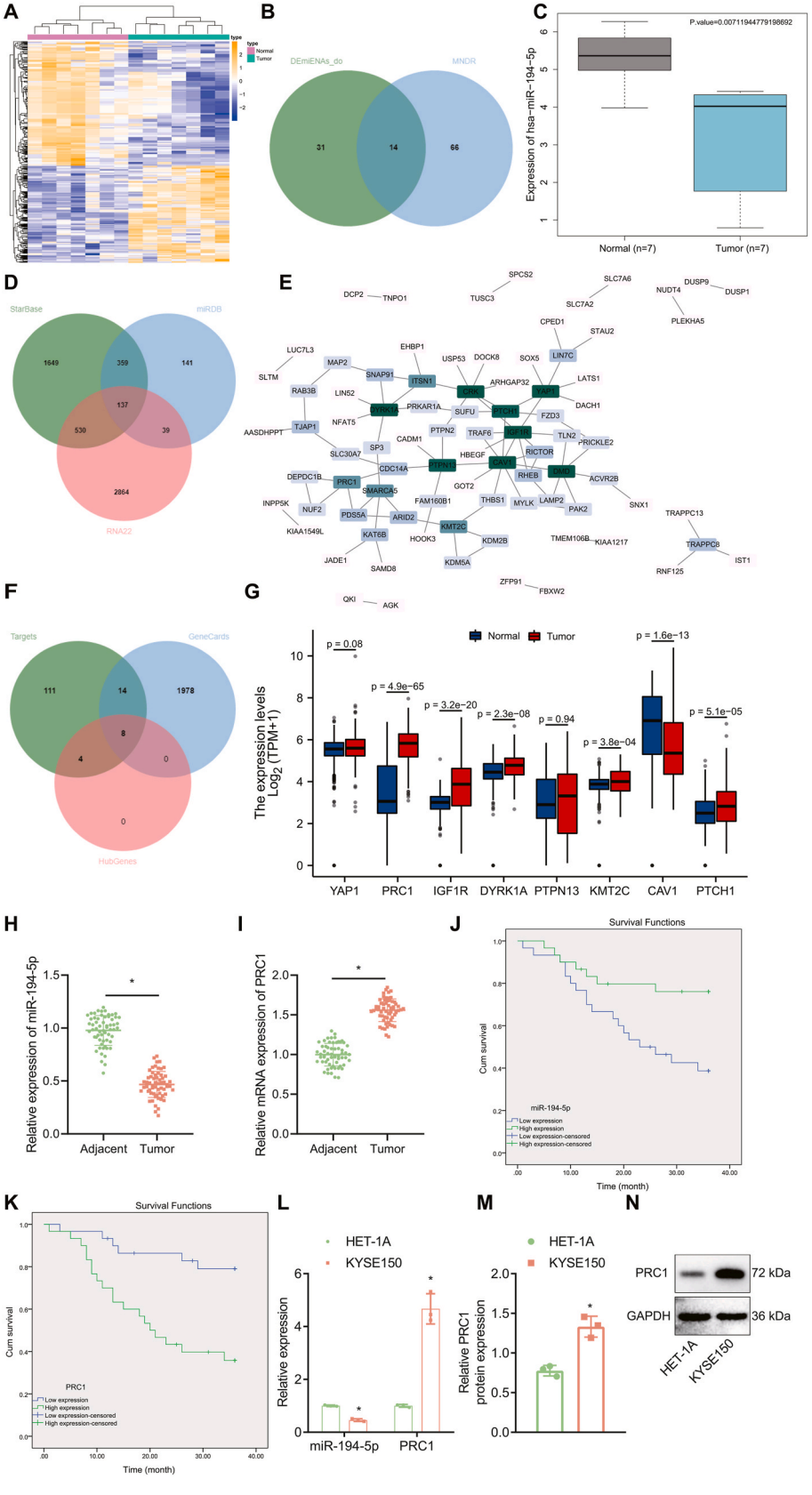

(caption on next page)

Fig. 1. Comprehensive microarray analysis identifies how miR-194-5p affects ESCC by regulating PRC1. A, Heat map of differentially expressed miRNA in ESCC-related expression microarray GSE97049 in GEO database, blue to orange expression values from small to large. B, Venn diagram of the intersection of differentially expressed and ESCC-related miRNAs in the MNDR database. C, Boxplots of miR-194-5p expression in GSE97049 microarray. D, Venn diagram of the intersection of the predicted target gene of miR-194-5p through StarBase database, miRDB database, and RNA22 database. E, PPI analysis network diagram of candidate target genes. The greener the color, the higher the Degree value and the higher the core degree. F, Venn diagram of intersection of candidate target genes, GeneCards database results, and Hub genes. G, Boxplots of gene expression (YAP1, PRC1, IGF1R, DYRK1A, PTPN13, KMT2C, CAV1, PTCH1) in normal samples (n = 666) and ESCC samples (n = 182). H. RT-qPCR detects the expression of miR-194-5p in the clinical group (n = 60); I. RT-qPCR detects the expression of PRC1 mRNA in clinical tissues (n = 60); J. Kaplan-Meier survival analysis esophageal squam Survival status of miR-194-5p expression in cancer; K. Kaplan-Meier survival analysis of PRC1 expression in esophageal squamous cell carcinoma; L, RT-qPCR determination of miR-194-5p and PRC1 expression in ESCC cells and normal esophageal epithelial cells. M, Statistics of protein expression in ESCC cells and normal esophageal epithelial cell line. N, Western blot analysis of PRC1 expression in ESCC cells and normal esophageal epithelial cell line. The data were expressed as the mean ± standard deviation, and data comparison between the two groups was conducted using a *t*-test. *p < 0.05 compared with adjacent non-tumor tissues or normal esophageal epithelial cell lines. The cell experiment was repeated three times.

mimic + oe-NC group, miR-194-5p mimic + oe-PRC1 group) were taken separately, trypsin digested, washed twice by centrifugation in PBS buffer and washed with cold PBS solution. The cell suspension was prepared, and the cell concentration was adjusted to 1 × 107 cells/mL; 0.4 % Typan blue staining was performed, and live cells were counted >98 %.

Tumor formation experiment in nude mice: 32 mice were randomly divided into 4 groups of 8 mice each, and 0.1 mL of the corresponding cell suspension was injected subcutaneously in the right axil of each group. The tumor formation was observed on days 7, 14, 21, 28, and 35 after successful subcutaneous injection, and the long diameter (a) and short diameter (b) of the tumor were measured and recorded using vernier calipers, and the volume was calculated using the formula = (a × b2)/2, and the tumor growth curve was plotted.

Nude mice metastasis model: 32 mice were randomly divided into 4 groups of 8 mice each, and 1×10^6 KYSE150 cells were injected into the tail vein of each group of nude mice to establish a nude mouse metastasis model. The mice were executed 35 days after tumor injection, and lung tissues were taken for H&E staining to detect metastatic foci.

2.15. H&E staining

The tumor tissue blocks were fixed, paraffin-embedded, sectioned (4 μm), dewaxed, stained with hematoxylin for 5 min, differentiated with hydrochloric acid for 30 s, and further stained with eosin for 2 min. Subsequently, cells were conventionally dehydrated, cleared, and sealed for observation under an inverted microscope (XSP-8CA, Shanghai Optical Instrument Factory, China).

2.16. Statistical analysis

Statistical data were processed and analyzed using SPSS 21.0 statistical software (SPSS, Inc., Chicago, IL, USA). The results of each parameter of the experimental measures were expressed as mean ± standard deviation (Mean ± SD). The data of cancerous and paraneoplastic tissues were analyzed by paired *t*-test, comparison between two groups was performed by *t*-test, and multiple groups were compared by analysis of variance (ANOVA) and Tukey for post hoc test. Two-factor ANOVA was used for cell activity/survival at different time points or doses and repeated-measures ANOVA was used for tumor volume at different times. Survival of miR-194-5p versus PRC1 expression in ESCC was analyzed by survival analysis using Kaplan-Meier with a test level of $\alpha = 0.05$, which was statistically significant when $P < 0.05$.

3. Results

3.1. Low expression of miR-194-5p and high expression of PRC1 in ESCC tissues and cells

The differential miRNA expression analysis of GSE97049, an ESCC-related expression microarray in the GEO database, yielded a total of 1359 differentially expressed miRNAs (Fig. 1A), including 131 miRNAs of human origin (86 highly expressed miRNAs and 45 lowly expressed miRNAs). Fifty-two miRNAs associated with ESCC were obtained from the MNDR database. To find potential miRNAs that inhibit ESCC, we intersected the differentially expressed miRNAs and MNDR results to obtain 11 candidate miRNAs (miR-133b, miR-29c-5p, miR-133a-3p, miR-139-5p miR-100-5p, miR-195-5p, miR-194-5p, miR-193a-3p, hsa-miR-133a-5p, hsa-miR-10a-5p, and hsa-miR-139-3p) (Fig. 1B). Further, we queried the literature on these miRNAs and ESCC, and the results showed that miR-194-5p was downregulated in ESCC tissues [13], which was the same as the results of GSE97049 microarray analysis (Fig. 1C).

To further predict the target genes of miR-194-5p, we obtained 2675, 676, and 3570 target genes of miR-194-5p using the StarBase database, miRDB database, and RNA22 database, respectively. We obtained 137 candidate genes by taking the overlapping part of each database (Fig. 1D). PPI analysis of candidate target genes was performed by GeneCards database of 2000 genes related to esophagus squamous cell carcinoma using STRING to obtain 12 core genes (Hub Gene, Degree>3) (Fig. 1E), taking the candidate target genes, The intersection of candidate target genes, GeneCards database results, and Hub genes were obtained for 8 genes (Fig. 1F). Next, we extracted the corresponding average tissue data from ESCA and GTEx of TCGA and analyzed the differential expression of the above eight genes (YAP1, PRC1, IGF1R, DYRK1A, PTPN13, KMT2C, CAV1, PTCH1), and the results showed that PRC1 was significantly

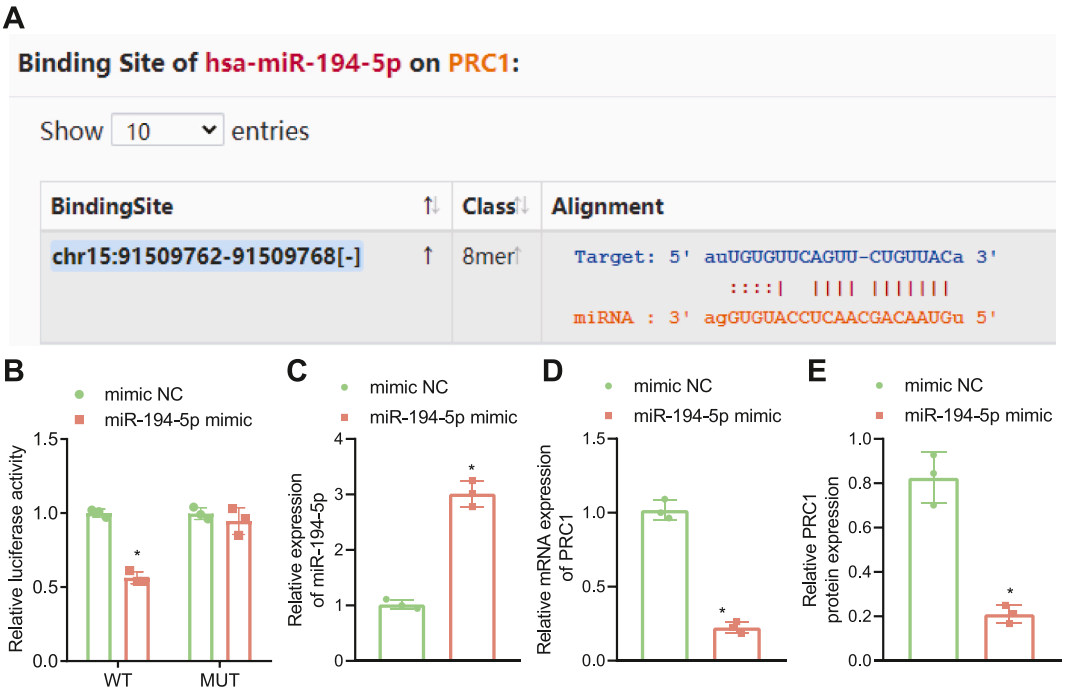

Fig. 2. PRC1 was a target gene of miR-194-5p. A, Binding site of miR-194-5p and PRC1 predicted by starBase. B, Binding of miR-194-5p to 3′-UTR of PCR1 verified by luciferase assay. C/D, RT-qPCR determination of miR-194-5p and PCR1 expression in KYSE150 cells. E, Western blot analysis of PCR1 expression in KYSE150 cells. *, $p < 0.05$, vs. mimic NC; The data were expressed as the mean ± standard deviation, and data comparison between two groups was conducted using *t*-test. The cell experiment was repeated three times.

highly expressed in ESCC with the most significant difference (Fig. 1G).

The expression levels of miR-194-5p and PRC1 were then measured in 60 patients with ESCC and their paraneoplastic tissues. The results showed that the expression of miR-194-5p was significantly lower ($P < 0.05$) in ESCC tissues compared with paraneoplastic tissues (Fig. 1H). The expression of PRC1 mRNA was significantly higher ($P < 0.05$) (Fig. 1I). In the survival analysis, patients with down-regulated miR-194-5p expression had a significantly lower survival rate (Fig. 1J). Those with up-regulated PRC1 expression had a lower survival rate (Fig. 1K). Similarly, we examined the expression levels of miR-194-5p and PRC1 in normal human esophageal epithelial cells HET-1A and ESCC cells KYSE150, and the results showed that the relative expression of miR-194-5p was significantly downregulated in ESCC cells KYSE150 compared with normal human esophageal epithelial cells HET-1A, the mRNA level of PRC1 was significantly The relative expression of miR-194-5p was significantly down-regulated, the mRNA level of PRC1 was significantly up-regulated, and the relative expression of PRC1 protein was also significantly up-regulated in KYSE150 esophageal cancer cells (Fig. 1L-N). The above results indicated that miR-194-5p showed low expression in ESCC cells, and PRC1 showed high expression in ESCC cells.

3.2. miR-194-5p targets and inhibits PRC1

To further investigate the specific regulatory mechanism of miR-194-5p and PRC1, we used StarBase prediction to find the binding site of miR-194-5p to the 3′UTR region of PRC1 (Fig. 2A). Dual luciferase reporter gene experiments showed that the luciferase signal was significantly decreased in the miR-194-5p mimic and pPRC1-wt co-transfected group compared to the NC group; no significant difference in luciferase signal was observed between the miR-194-5p mimic and pPRC1-mut co-transfected groups ($P > 0.05$) (Fig. 2B). Further, miR-194-5p was overexpressed in KYSE150 cells, and RT-qPCR assay showed that miR-194-5p miR-194-5p expression was significantly increased in the miR-194-5p mimic group compared with the mimic NC group ($P < 0.05$, Fig. 2C). RT-qPCR and Western blot The results showed that both mRNA and protein levels of PCR1 were significantly decreased in the miR-194-5p mimic group compared with the mimic NC group ($P < 0.05$, Fig. 2D and E). The above results indicated that miR-194-5p could specifically inhibit the expression of PRC1.

3.3. Upregulation of miR-194-5p or silencing PRC1 enhances sensitivity to radiotherapy and inhibits the proliferation of ESCC cells in nasopharyngeal carcinoma

To detect the effects of miR-194-5p and PCR1 on the migration and invasion ability of ESCC cells, we first treated KYSE150 cells with PRC1 silencing, miR-194-5p overexpression or both miR-194-5p and PRC1. The knockdown treatment of PRC1 using shRNA and RT-qPCR to detect the silencing efficiency of both shRNAs showed that the knockdown efficiency of sh-PRC1-1 was high for the follow-

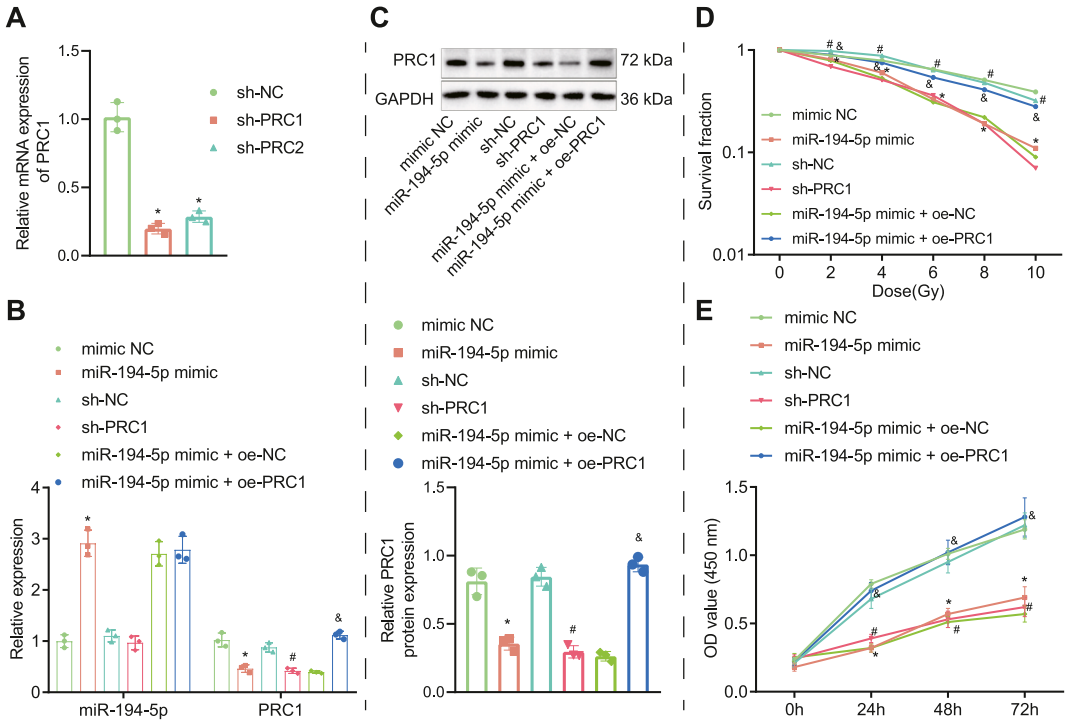

Fig. 3. Overexpressed miR-194-5p or silenced PRC1 enhanced radiosensitivity but retarded proliferation of ESCC cells. A, RT-qPCR determination of PRC1 expression after sh-PRC1 treatment. KYSE150 cells were transfected with miR-194-5p mimic, sh-PRC1, or oe-PRC1. B, RT-qPCR determination of miR-194-5p and PRC1 expression in each group of cells. C, Western blot analysis of PRC1 expression in each group of cells. D, Clone formation assay was used to detect cell survival rate. E, CCK-8 assay was performed to assess cell proliferation. The data were expressed as the mean ± standard deviation, and data comparison between multiple groups was conducted using two-way ANOVA. *, $p < 0.05$, vs mimic NC; #, $p < 0.05$, vs sh-NC; &, $p < 0.05$, vs miR-194-5p mimic + oe-NC. The cell experiment was repeated three times.

up study ($P < 0.05$, Fig. 3A). RT-qPCR was performed to detect the miR-194-5p and PRC1 mRNA in each group of KYSE150 cells expression. WB detected PRC1 protein expression in KYSE150 cells in each group. The results showed (Fig. 3B and C): compared with the mimic NC group, miR-194-5p miR-194-5p expression was significantly increased, and PRC1 expression was decreased in the mimic group; compared with the sh-NC group, miR-194-5p expression in the sh-PRC1 group was not significantly different, and PRC1 expression decreased; compared with miR-194-5p mimic + oe-NC group, miR-194-5p mimic + oe-PRC1 group miR-194-5p expression was not significantly different and PRC1 expression increased.

The effect of radiotherapy on in vitro cell survival was examined using in vitro clone formation assay, and the results showed (Fig. 3D): with increasing intensity of radiotherapy, the KYSE150 cell survival rate in the miR-194-5p mimic group was significantly decreased compared with the mimic NC group; the KYSE150 cell survival rate in the sh-PRC1 group was significantly decreased compared with the sh-NC group; The survival rate of KYSE150 cells in the miR-194-5p mimic + oe-NC group was significantly increased compared with the miR-194-5p mimic + oe-PRC1 group. The results suggest that overexpression of miR-194-5p or silencing of PRC1 increased cellular radiosensitivity.

CCK-8 detected the proliferation of KYSE150 cells, and the results showed (Fig. 3E): that compared with the mimic NC group, the relative viability of KYSE150 cells in the miR-194-5p mimic group was significantly reduced, and the proliferation rate slowed down after 24 h, 48 h and 72 h of culture; compared with the sh-NC group, the sh-PRC1 group The relative viability of KYSE150 cells was significantly reduced, and the proliferation rate was slowed down; compared with the miR-194-5p mimic + oe-NC group, the relative viability of KYSE150 cells in the miR-194-5p mimic + oe-PRC1 group was significantly increased, and the proliferation rate was accelerated.

The above results suggest that overexpression of miR-194-5 p or silencing PRC1 can enhance chemosensitivity and inhibit the proliferation of ESCC cells, while overexpression of PRC1 can reverse the inhibitory effect of miR-194-5 overexpression on the proliferation of ESCC cells.

3.4. Upregulation of miR-194-5p or silencing PRC1 inhibits migration and invasion of ESCC cells, blocks cell cycle progression, and promotes apoptosis

The results of scratch and Transwell assays demonstrated that mimic of miR-194-5p or sh-PRC1 suppressed cell invasion and migration at 48 h, while relative to miR-194-5p mimic + oe-NC treatment, both miR-194-5p mimic and oe-PRC1 treatment enhanced

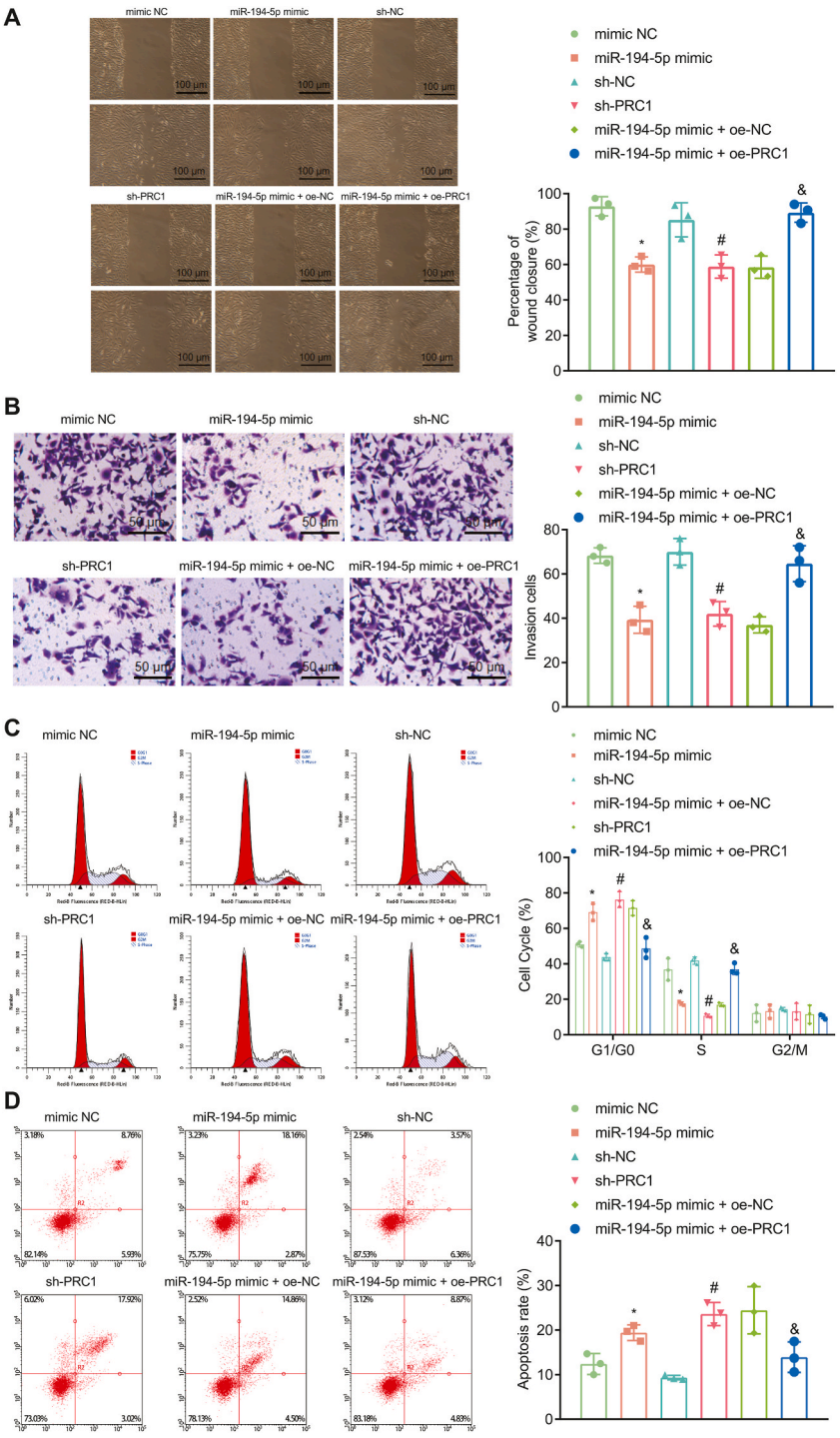

Fig. 4. Overexpressed miR-194-5p or silenced PRC1 represses invasion and migration of ESCC cells but induces apoptosis. KYSE150 cells were transfected with miR-194-5p mimic, sh-PRC1, or oe-PRC1. A, The migration of KYSE150 cells was assessed by scratch test (100 μm). B, The cell invasion was assessed by Transwell assay (50 μm). C, The cell cycle was assessed by flow cytometry. D, The cell apoptosis was determined by flow cytometry. The data were expressed as the mean ± standard deviation, and data comparison between multiple groups was conducted using two-way ANOVA. *, $p < 0.05$, vs mimic NC; #, $p < 0.05$, vs sh-NC; &, $p < 0.05$, vs miR-194-5p mimic + oe-NC. The cell experiment was repeated three times.

cell invasion and migration (Fig. 4A and B).

Further cell cycle distribution and cell apoptosis analysis indicated that miR-194-5p mimic or sh-PRC1 treatment increased the percentage of G1-phase cells and cell apoptosis but reduced that of S-phase cells relative to miR-194-5p mimic + oe-NC treatment, both

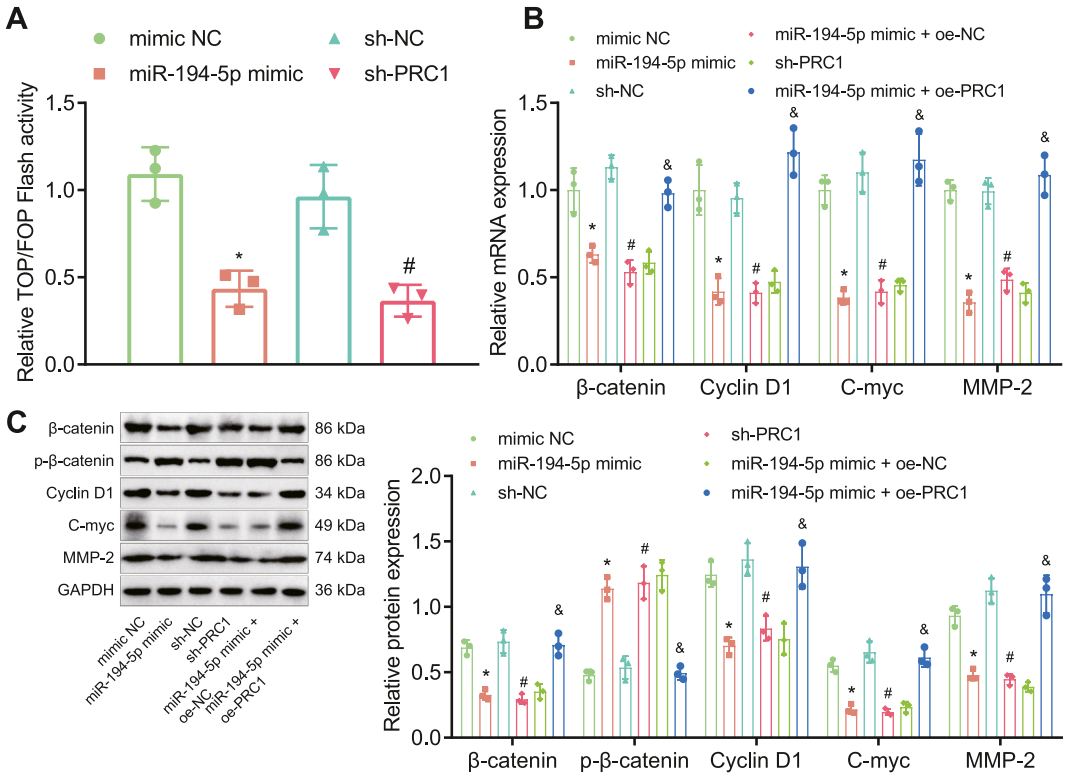

Fig. 5. miR-194-5p regulates the Wnt/β-catenin signaling pathway by targeting PRC1. A TOP/FOP luciferase assay detects the TOP/FOP ratio after miR-194-5p mimic or sh-PRC1 treatment. B/C, RT-qPCR, and Western blot analysis of the expression of p-β-catenin, β-catenin, Cyclin D1, C-myc, and MMP-2 mRNA in KYSE150 cells after miR-194-5p mimic, oe-PRC1, or sh-PRC1 treatment. The data were presented as the mean ± standard deviation, and data comparison between multiple groups was conducted using one-way ANOVA followed by Turkey post hoc test. *, $p < 0.05$, vs mimic NC; #, $p < 0.05$, vs sh-NC; &, $p < 0.05$, vs miR-194-5p mimic + oe-NC. The cell experiment was repeated three times.

miR-194-5p mimic and oe-PRC1 treatment reduced the percent of G1-phase cells and cell apoptosis but increased that of S-phase cells (Fig. 4C and D).

The above results suggest that overexpression of miR-194-5p or silencing PRC1 can inhibit the migration and invasion of ductal carcinoma cells, while overexpression of PRC1 can reverse the inhibitory effect of miR-194-5 overexpression on the biological properties of ESCC cells.

3.5. *miR-194-5p targets PRC1 to mediate the Wnt/β-catenin signaling pathway*

Further literature search on the function of PRC1 found that PRC1 can affect the disease process through the Wnt/β-catenin signaling pathway [21–23]. To further examine the effect of miR-194-5p and PRC1 on the Wnt/β-catenin signaling pathway, we conducted TOP/FOP luciferase assay and found that (Fig. 5A) treatment of miR-194-5p mimic or sh-PRC1 significantly decreased the TOP/FOP ratio, suggesting that hsa-miR-194-5p could target PRC1 to regulate Wnt/β-catenin signaling pathway, thereby inhibiting the development of ESCC. Furthermore, qPCR and Western blot analysis showed that treatment of miR-194-5p mimic or sh-PRC1 markedly reduced the expression of β-catenin, Cyclin D1, C-myc, and MMP-2 mRNA and protein but increased the expression of p-β-catenin; relative to miR-194-5p mimic + oe-NC treatment, both miR-194-5p mimic and oe-PRC1 treatment elevated the expression of β-catenin, Cyclin D1, C-myc, and MMP-2 mRNA and protein but diminished the expression of p-β-catenin (Fig. 5B and C). These results supported the suppressive role of miR-194-5p in ESCC via reducing PRC1 expression through the Wnt/β-catenin signaling pathway.

3.6. *Upregulation of miR-194-5p inhibits xenograft tumorigenesis and lymph node metastasis in nude mice*

Next, we processed the experiment in nude mice, aiming to evaluate the impact of miR-194-5p and PRC1 on the in vivo tumor growth of ESCC. The tumor volume was calculated, a growth curve was made (Fig. 6A), and the tumor weight was weighed by an electronic balance (Fig. 6B and C). The tumor volume and weight were reduced in mice injected with miR-194-5p mimic, while further injection of oe-PRC1 led to the opposite trend.

Further, the effect of miR-194-5p on metastasis was also observed. HE staining results (Fig. 6D–F) confirmed that treatment of miR-

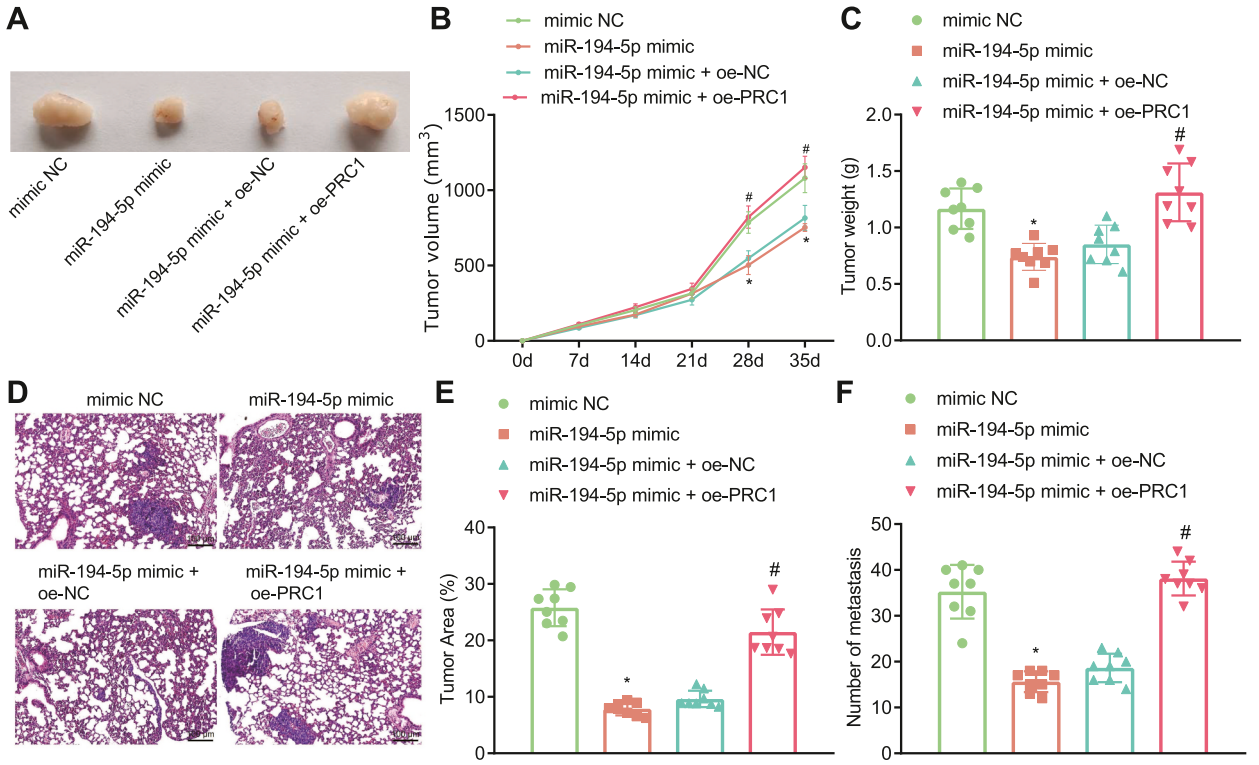

Fig. 6. Elevation of miR-194-5p or silenced PRC1 suppresses xenograft growth and metastasis in ESCC mice. A, Tumor volume after miR-194-5p mimic or oe-PRC1 treatment. B, Tumor weight after miR-194-5p mimic or oe-PRC1treatment. C, Representative maps of xenografts after miR-194-5p mimic or oe-PRC1 treatment. D, HE staining results of xenografts after miR-194-5p mimic or oe-PRC1 treatment (100 μm). E, The area of lung tissue metastases in nude mice models of metastasis in each group after miR-194-5p mimic or oe-PRC1 treatment. F, Statistical chart of lung metastases in each group's nude mouse metastasis models. n = 8. *, $p < 0.05$, vs mimic NC; #, $p < 0.05$, vs miR-194-5p mimic + oe-NC.

194-5p mimics reduced the area and a number of metastases in the lung tissue of nude mice, which could be reversed by further oe-PRC1 injection. This evidence indicated that upregulation of miR-194-5p inhibited PRC1, inhibiting tumorigenesis and in vivo metastasis in nude mice.

4. Discussion

ESCC is a common malignancy, and its highly malignant invasive and metastatic process is one of the major causes of poor prognosis [24]. In recent years, more and more studies have shown that miRNAs play an essential regulatory role in tumor invasion and metastasis, thus becoming a hot spot for many tumor studies [25]. In the present study, miR-194-5p was found to inhibit the Wnt/β-catenin signaling pathway through the down-regulation of the PRC1 gene, which in turn enhanced the sensitivity of ESCC cells to radiotherapy and attenuated the invasion and metastasis ability of ESCC cells.

Based on bioinformatics analysis and clinical tissue and cellular experiments, we found that miR-194-5p expression was low in ESCC tissues and cells, and its high expression was able to inhibit ESCC cell proliferation, invasion, and migration but enhance the radiosensitivity of ESCC cells. There is increasing evidence that miR-194-5p has tumor-suppressive effects in various cancers such as hepatocellular carcinoma, breast cancer, and Wilms' tumor [26,27]. Consistent with our study, recent reports have also demonstrated the downregulation of miR-194-5p expression in ESCC [13]. More importantly, miR-194 was shown to limit the proliferation and invasion of ESCC cells and promote their apoptosis [28]. miRBase Sanger sequences revealed that miR-194-5p and miR-194-3p are two mature sequences of miR-194 [29]. A recent study revealed that overexpression of miR-194-3p can enhance sensitivity to radiotherapy and inhibit cell migration, invasion, and proliferation in nasopharyngeal carcinoma [30].

In addition, high expression of PRC1 was also detected in ESCC tissues and cells, and its downregulation could limit the proliferation, invasion, and migration of ESCC cells but could enhance the radiosensitivity of ESCC cells. PRC1 is a suitable substrate for activating CDKs and plays a crucial role in cell division and tumorigenesis [31]. A study showed that overexpression of PRC1 may contribute to gastric carcinogenesis [32]. Cai et al. consistently summarized the upregulated expression of PRC1 in esophageal cancer, and its low expression prevented proliferation, invasion, and self-renewal of esophageal cancer stem cells [33].

miRNAs are endogenous, non-coding, single-stranded RNAs that play essential roles in different biological processes by binding to their target mRNAs [34]. Our study also confirmed that miR-194-5p can target PRC1 expression and reduce PRC1 expression by blocking the Wnt/β-catenin signaling pathway, leading to the inhibitory effect of miR-194-5p in ESCC. Specifically, miR-194-5p

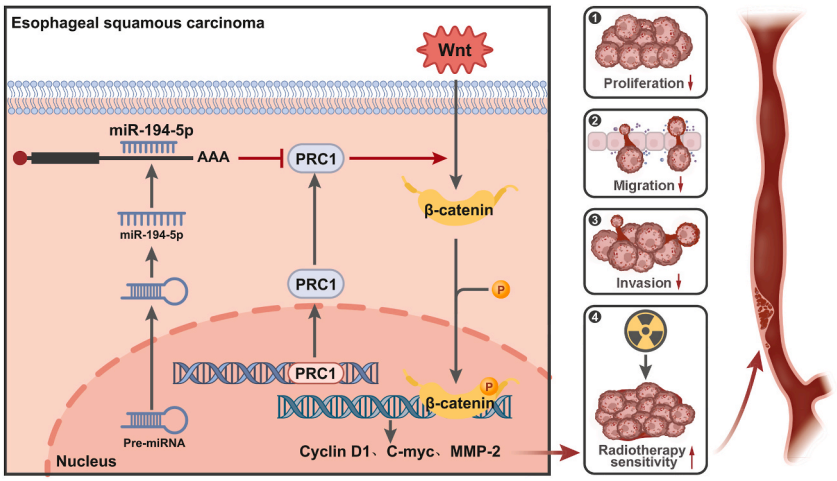

Fig. 7. Molecular mechanism of miR-194-5p/PRC1/Wnt/β-catenin axis affecting invasion, metastasis, and radiosensitivity of ESCC cells. miR-194-5p can inhibit the Wnt/β-catenin signaling pathway by targeting the expression of PRC1, thereby enhancing the radiosensitivity of ESCC cells and attenuating the invasion and metastasis of ESCC cells.

overexpression or PRC1 downregulation inhibits the expression of β-catenin, Cyclin D1, C-myc, and MMP-2. The Wnt/β-catenin signaling pathway is an evolutionarily conserved pathway that has been shown to promote tumorigenesis and metastasis in certain cancers, including ESCC [35,36]. Aberrant activation of the Wnt/β-catenin signaling pathway leads to the accumulation of β-catenin in the nucleus, which promotes the transcription of many oncogenes, such as C-myc, CyclinD1 and MMP-2 [37–39]. Previous studies have found that PRC1 increases lymph node metastasis in lung adenocarcinoma by activating the Wnt/β-catenin signaling pathway [21]. PRC1 is associated with developing diseases associated with regulating the Wnt/β-catenin signaling pathway [40]. In partial agreement with our study, Tang et al. also demonstrated a target site relationship between miR-194 and PRC1, and that increased miR-194 produced inhibitory effects in hepatocellular carcinoma cells by blocking the Wnt/β-catenin signaling pathway, including inhibition of epithelial-mesenchymal transition, growth, proliferation, invasion, and migration [33]. In addition, a recently published study also validated the targeting relationship between miR-194 and PRC1 in esophageal cancer and that miR-194 may reduce PRC1 expression through the inactivation of the Wnt/β-catenin signaling pathway, thereby preventing tumorigenesis in esophageal cancer stem cells, which is highly consistent with our current findings [33].

Firstly, it should be noted that this study only conducted experiments in cell cultures and nude mouse models, lacking clinical sample data support. Furthermore, the cell lines used in this study were heterogeneous, and the radiosensitivity could vary among different cell lines. Additionally, differences between the in vitro culture conditions and the tumor growth environment may exist. Secondly, miR-194-5p and PRC1 may also play essential roles in other types of tumors. Therefore, further investigation is needed to determine whether the effects of these regulatory factors are specific to esophageal squamous cell carcinoma cells. Lastly, this study revealed the involvement of miR-194-5p and PRC1 in regulating the radiosensitivity of esophageal squamous cell carcinoma cells. However, the occurrence and development of esophageal squamous cell carcinoma is a complex, multi-gene regulatory process, and the mechanisms underlying radiosensitivity are not fully understood. Therefore, further research is warranted to explore other vital regulatory genes and signaling pathways. We will also endeavor to delve deeper into the topic in future studies.

5. Conclusion

This study investigated the molecular mechanism of miR-194-5p/PRC1/Wnt/β-catenin signaling axis to regulate the invasion and metastatic ability and sensitivity to radiotherapy in ESCC cells. The results showed that miR-194-5p could inhibit the Wnt/β-catenin signaling pathway through the down-regulation of the PRC1 gene to improve the sensitivity of ESCC cells to radiotherapy and reduce their invasion and metastatic ability (Fig. 7). Therefore, this study has significant scientific and clinical implications for the treatment of ESCC. However, there are limitations to this study. First, the study was conducted only in cellular experiments and nude mouse models and lacked data support from clinical samples. Second, the study did not consider other influencing factors, such as miRNAs and gene regulation.

Ethics approval and consent to participate

All patients signed an informed consent form, which our clinical ethics committee approved and agreed upon, and all specimens were used following the Declaration of Helsinki. All experimental operations followed the International Convention on Laboratory Animal Ethics and met relevant national regulations.

Consent for publication

Consent for publication was obtained from the participants.

Funding statement

Not applicable.

Data availability statement

Data included in article/supp. material/referenced in article.

CRediT authorship contribution statement

Yan Wang: Writing – review & editing, Writing – original draft, Resources, Methodology, Investigation, Formal analysis, Data curation, Conceptualization. **Ninghua Yao:** Writing – review & editing, Writing – original draft, Software, Methodology, Investigation, Data curation, Conceptualization. **Jie Sun:** Writing – review & editing, Writing – original draft, Validation, Methodology, Investigation, Funding acquisition, Formal analysis, Data curation, Conceptualization.

Declaration of competing interest

The authors declare that they have no competing interests.

Acknowledgement

Not applicable.

Appendix A. Supplementary data

Supplementary data to this article can be found online at https://doi.org/10.1016/j.heliyon.2023.e22282.

Abbreviations

ESCC	Esophageal squamous cell carcinoma
PRC1	Polycomb complex 1
WT	wild-type
SF	surviving fraction
ANOVA	analysis of variance

References

[1] Y.K. Kang, L.T. Chen, M.H. Ryu, D.Y. Oh, S.C. Oh, H.C. Chung, et al., Nivolumab plus chemotherapy versus placebo plus chemotherapy in patients with HER2-negative, untreated, unresectable advanced or recurrent gastric or gastro-oesophageal junction cancer (ATTRACTION-4): a randomised, multicentre, double-blind, placebo-controlled, phase 3 trial, Lancet Oncol. 23 (2) (2022) 234–247, https://doi.org/10.1016/S1470-2045(21)00692-6.

[2] M. Tian, R. Zhu, F. Ding, Z. Liu, Ubiquitin-specific peptidase 46 promotes tumor metastasis through stabilizing ENO1 in human esophageal squamous cell carcinoma, Exp. Cell Res. 395 (1) (2020), 112188, https://doi.org/10.1016/j.yexcr.2020.112188.

[3] Y. Chen, S. Zhu, T. Liu, S. Zhang, J. Lu, W. Fan, et al., Epithelial cells activate fibroblasts to promote esophageal cancer development, Cancer Cell 41 (5) (2023) 903–918 e908, https://doi.org/10.1016/j.ccell.2023.03.001.

[4] H. Scherubl, [Smoking tobacco and cancer risk], Dtsch. Med. Wochenschr. 146 (6) (2021) 412–417, https://doi.org/10.1055/a-1216-7050.

[5] C. Chen, L. Xie, T. Ren, Y. Huang, J. Xu, W. Guo, Immunotherapy for osteosarcoma: fundamental mechanism, rationale, and recent breakthroughs, Cancer Lett. 500 (2021) 1–10, https://doi.org/10.1016/j.canlet.2020.12.024.

[6] X. Li, L. Chen, S. Luan, J. Zhou, X. Xiao, Y. Yang, et al., The development and progress of nanomedicine for esophageal cancer diagnosis and treatment, Semin. Cancer Biol. 86 (Pt 2) (2022) 873–885, https://doi.org/10.1016/j.semcancer.2022.01.007.

[7] L. Walcher, A.K. Kistenmacher, H. Suo, R. Kitte, S. Dluczek, A. Strauss, et al., Cancer stem cells-origins and biomarkers: perspectives for targeted personalized therapies, Front. Immunol. 11 (2020) 1280, https://doi.org/10.3389/fimmu.2020.01280.

[8] Y. Chen, G. Tang, H. Qian, J. Chen, B. Cheng, C. Zhou, et al., LncRNA LOC100129620 promotes osteosarcoma progression through regulating CDK6 expression, tumor angiogenesis, and macrophage polarization, Aging (Albany NY) 13 (10) (2021) 14258–14276, https://doi.org/10.18632/aging.203042.

[9] M. Santoni, A. Rizzo, V. Mollica, M.R. Matrana, M. Rosellini, L. Faloppi, et al., The impact of gender on the efficacy of immune checkpoint inhibitors in cancer patients: the MOUSEION-01 study, Crit. Rev. Oncol. Hematol. 170 (2022), 103596, https://doi.org/10.1016/j.critrevonc.2022.103596.

[10] K. Rihawi, A.D. Ricci, A. Rizzo, S. Brocchi, G. Marasco, L.V. Pastore, et al., Tumor-associated macrophages and inflammatory microenvironment in gastric cancer: novel translational implications, Int. J. Mol. Sci. 22 (8) (2021), https://doi.org/10.3390/ijms22083805.

[11] M. Santoni, A. Rizzo, J. Kucharz, V. Mollica, M. Rosellini, A. Marchetti, et al., Complete remissions following immunotherapy or immuno-oncology combinations in cancer patients: the MOUSEION-03 meta-analysis, Cancer Immunol. Immunother. 72 (6) (2023) 1365–1379, https://doi.org/10.1007/s00262-022-03349-4.

[12] Z. Xie, C. Zhong, S. Duan, miR-1269a and miR-1269b: emerging carcinogenic genes of the miR-1269 family, Front. Cell Dev. Biol. 10 (2022), 809132, https://doi.org/10.3389/fcell.2022.809132.
[13] F. Qu, L. Wang, C. Wang, L. Yu, K. Zhao, H. Zhong, Circular RNA circ_0006168 enhances Taxol resistance in esophageal squamous cell carcinoma by regulating miR-194-5p/JMJD1C axis, Cancer Cell Int. 21 (1) (2021) 273, https://doi.org/10.1186/s12935-021-01984-y.
[14] M. Meijer, E. Agirre, M. Kabbe, C.A. Van Tuijn, A. Heskol, C. Zheng, et al., Epigenomic priming of immune genes implicates oligodendroglia in multiple sclerosis susceptibility, Neuron 110 (7) (2022) 1193–1210 e1113, https://doi.org/10.1016/j.neuron.2021.12.034.
[15] G.J. Dong, J.L. Xu, Y.R. Qi, Z.Q. Yuan, W. Zhao, Critical roles of Polycomb repressive complexes in transcription and cancer, Int. J. Mol. Sci. 23 (17) (2022), https://doi.org/10.3390/ijms23179574.
[16] J. Shi, S. Hao, X. Liu, Y. Li, X. Zheng, Feiyiliu Mixture sensitizes EGFR(Del19/T790M/C797S) mutant non-small cell lung cancer to osimertinib by attenuating the PRC1/Wnt/EGFR pathway, Front. Pharmacol. 14 (2023), 1093017, https://doi.org/10.3389/fphar.2023.1093017.
[17] M. Wiese, N. Walther, C. Diederichs, F. Schill, S. Monecke, G. Salinas, et al., The beta-catenin/CBP-antagonist ICG-001 inhibits pediatric glioma tumorigenicity in a Wnt-independent manner, Oncotarget 8 (16) (2017) 27300–27313, https://doi.org/10.18632/oncotarget.15934.
[18] J. Liu, Q. Xiao, J. Xiao, C. Niu, Y. Li, X. Zhang, et al., Wnt/beta-catenin signalling: function, biological mechanisms, and therapeutic opportunities, Signal Transduct. Targeted Ther. 7 (1) (2022) 3, https://doi.org/10.1038/s41392-021-00762-6.
[19] B. Mi, C. Yan, H. Xue, L. Chen, A.C. Panayi, L. Hu, et al., Inhibition of circulating miR-194-5p reverses osteoporosis through wnt5a/beta-catenin-dependent induction of osteogenic differentiation, Mol. Ther. Nucleic Acids 21 (2020) 814–823, https://doi.org/10.1016/j.omtn.2020.07.023.
[20] A.N. Alexopoulou, M. Leao, O.L. Caballero, L. Da Silva, L. Reid, S.R. Lakhani, et al., Dissecting the transcriptional networks underlying breast cancer: NR4A1 reduces the migration of normal and breast cancer cell lines, Breast Cancer Res. 12 (4) (2010) R51, https://doi.org/10.1186/bcr2610.
[21] P. Zhan, B. Zhang, G.M. Xi, Y. Wu, H.B. Liu, Y.F. Liu, et al., PRC1 contributes to tumorigenesis of lung adenocarcinoma in association with the Wnt/beta-catenin signaling pathway, Mol. Cancer 16 (1) (2017) 108, https://doi.org/10.1186/s12943-017-0682-z.
[22] J. Chen, M. Rajasekaran, H. Xia, X. Zhang, S.N. Kong, K. Sekar, et al., The microtubule-associated protein PRC1 promotes early recurrence of hepatocellular carcinoma in association with the Wnt/beta-catenin signalling pathway, Gut 65 (9) (2016) 1522–1534, https://doi.org/10.1136/gutjnl-2015-310625.
[23] F. Chiacchiera, A. Rossi, S. Jammula, A. Piunti, A. Scelfo, P. Ordonez-Moran, et al., Polycomb complex PRC1 preserves intestinal stem cell identity by sustaining wnt/beta-catenin transcriptional activity, Cell Stem Cell 18 (1) (2016) 91–103, https://doi.org/10.1016/j.stem.2015.09.019.
[24] D. Mei, Y. Zhu, L. Zhang, W. Wei, The role of CTHRC1 in regulation of multiple signaling and tumor progression and metastasis, Mediat. Inflamm. 2020 (2020), 9578701, https://doi.org/10.1155/2020/9578701.
[25] C. Amri, A.K. Shukla, J.H. Lee, Recent advancements in nanoparticle-based optical biosensors for circulating cancer biomarkers, Materials 14 (6) (2021), https://doi.org/10.3390/ma14061339.
[26] S. Ghafouri-Fard, T. Khoshbakht, B.M. Hussen, M. Taheri, M. Samadian, A review on the role of MCM3AP-AS1 in the carcinogenesis and tumor progression, Cancer Cell Int. 22 (1) (2022) 225, https://doi.org/10.1186/s12935-022-02644-5.
[27] M. Zhou, H. Cheng, Y. Fu, J. Zhang, Long noncoding RNA DARS-AS1 regulates TP53 ubiquitination and affects ovarian cancer progression by modulation miR-194-5p/RBX1 axis, J. Biochem. Mol. Toxicol. 35 (10) (2021), e22865, https://doi.org/10.1002/jbt.22865.
[28] G. Liang, H. Wang, H. Shi, M. Zhu, J. An, Y. Qi, et al., Porphyromonas gingivalis promotes the proliferation and migration of esophageal squamous cell carcinoma through the miR-194/GRHL3/PTEN/akt Axis, ACS Infect. Dis. 6 (5) (2020) 871–881, https://doi.org/10.1021/acsinfecdis.0c00007.
[29] H. Yang, C. Zhang, Anti-epileptic effect of 2-deoxy-D-glucose by activation of miR-194/K(ATP) signaling pathway, Zhong Nan Da Xue Xue Bao Yi Xue Ban 47 (8) (2022) 1099–1107, https://doi.org/10.11817/j.issn.1672-7347.2022.220111.
[30] L. Yi, L. Ouyang, S. Wang, S.S. Li, X.M. Yang, Long noncoding RNA PTPRG-AS1 acts as a microRNA-194-3p sponge to regulate radiosensitivity and metastasis of nasopharyngeal carcinoma cells via PRC1, J. Cell. Physiol. 234 (10) (2019) 19088–19102, https://doi.org/10.1002/jcp.28547.
[31] R.T. Perchey, M.P. Serres, A. Nowosad, J. Creff, C. Callot, A. Gay, et al., p27(Kip1) regulates the microtubule bundling activity of PRC1, Biochim. Biophys. Acta Mol. Cell Res. 1865 (11 Pt A) (2018) 1630–1639, https://doi.org/10.1016/j.bbamcr.2018.08.010.
[32] J R M V S, BMI1 and PTEN are key determinants of breast cancer therapy: a plausible therapeutic target in breast cancer, Gene 678 (2018) 302–311, https://doi.org/10.1016/j.gene.2018.08.022.
[33] S. Cai, Y. Weng, F. Miao, MicroRNA-194 inhibits PRC1 activation of the Wnt/beta-catenin signaling pathway to prevent tumorigenesis by elevating self-renewal of non-side population cells and side population cells in esophageal cancer stem cells, Cell Tissue Res. 384 (2) (2021) 353–366, https://doi.org/10.1007/s00441-021-03412-z.
[34] L. Cai, D. Lai, J. Gao, H. Wu, B. Shi, H. Ji, et al., The role and mechanisms of miRNA in neonatal necrotizing enterocolitis, Front Pediatr 10 (2022), 1053965, https://doi.org/10.3389/fped.2022.1053965.
[35] N. Krishnamurthy, R. Kurzrock, Targeting the Wnt/beta-catenin pathway in cancer: update on effectors and inhibitors, Cancer Treat Rev. 62 (2018) 50–60, https://doi.org/10.1016/j.ctrv.2017.11.002.
[36] Y. Zhang, X. Wang, Targeting the Wnt/beta-catenin signaling pathway in cancer, J. Hematol. Oncol. 13 (1) (2020) 165, https://doi.org/10.1186/s13045-020-00990-3.
[37] X. Liu, X. Zuo, X. Sun, X. Tian, Y. Teng, Hexokinase 2 promotes cell proliferation and tumor formation through the wnt/beta-catenin pathway-mediated Cyclin D1/c-myc upregulation in epithelial ovarian cancer, J. Cancer 13 (8) (2022) 2559–2569, https://doi.org/10.7150/jca.71894.
[38] H. You, D. Wang, L. Wei, J. Chen, H. Li, Y. Liu, Deferoxamine inhibits acute lymphoblastic leukemia progression through repression of ROS/HIF-1alpha, wnt/beta-catenin, and p38MAPK/ERK pathways, J Oncol 2022 (2022), 8281267, https://doi.org/10.1155/2022/8281267.
[39] X. Fan, X. Niu, Z. Wu, L. Yao, S. Chen, W. Wan, et al., Computer image analysis reveals C-myc as a potential biomarker for discriminating between keratoacanthoma and cutaneous squamous cell carcinoma, BioMed Res. Int. 2022 (2022), 3168503, https://doi.org/10.1155/2022/3168503.
[40] N.P. Blackledge, R.J. Klose, The molecular principles of gene regulation by Polycomb repressive complexes, Nat. Rev. Mol. Cell Biol. 22 (12) (2021) 815–833, https://doi.org/10.1038/s41580-021-00398-y.